Ge–SiGe Quantum-Well Waveguide Photodetectors on Silicon for the Near-Infrared

Onur Fidaner, Student Member, IEEE, Ali K. Okyay, Student Member, IEEE, Jonathan E. Roth, Student Member, IEEE, Rebecca K. Schaevitz, Yu-Hsuan Kuo, Krishna C. Saraswat, Fellow, IEEE, James S. Harris, Jr., Fellow, IEEE, and David A. B. Miller, Fellow, IEEE

Abstract—We demonstrate near-infrared waveguide photodetectors using Ge–SiGe quantum wells epitaxially grown on a silicon substrate. The diodes exhibit a low dark current of 17.9 mA/cm^2 at 5-V reverse bias. The photodetectors are designed to work optimally at ~1480 nm, where the external responsivity is 170 mA/W, which is mainly limited by the fiber-to-waveguide coupling loss. The ~1480-nm wavelength matches the optimum wavelength for quantum-well electroabsorption modulators built on the same epitaxy, but these photodetectors also exhibit performance comparable to the demonstrated Ge-based detectors at longer wavelengths. At 1530 nm, we see open eye diagrams at 2.5-Gb/s operation and the external responsivity is as high as 66 mA/W. The technology is potentially integrable with the standard complementary metal–oxide–semiconductor process and offers an efficient solution for on-chip optical interconnects.

Index Terms—Integrated optoelectronics, near-infrared photodetectors, quantum wells, silicon–germanium (SiGe), silicon optoelectronics.

I. INTRODUCTION

OPTICAL interconnects have been evaluated as an efficient alternative to electrical interconnects on silicon. Recently, germanium and silicon–germanium-based photodetectors have drawn attention for the receiver end of optical interconnects since these group IV materials can be grown on silicon, allowing for monolithic integration of detectors with the silicon complementary metal–oxide–semiconductor (CMOS) technology. These detectors are also promising alternatives to InGaAs-based detectors for ~1550-nm detection since they can be monolithically integrated with the CMOS receiver circuit [1]–[6].

Most of the recent demonstrations of germanium or silicon–germanium detectors include either a normal incidence p-i-n mesa structure or a metal–semiconductor–metal structure. A p-i-n structure with 39-GHz bandwidth and a resonant-cavity enhanced structure with 59% external quantum efficiency have been reported at 1550-nm operation [1], [3]. A

O. Fidaner, A. K. Okyay, J. E. Roth, R. K. Schaevitz, K. C. Saraswat, J. S. Harris, Jr., and D. A. B. Miller are with the Department of Electrical Engineering, Stanford University, Stanford, CA 94305 USA (e-mail: ofidaner@stanfordalumni.org).

Y.-H. Kuo was with the Department of Electrical Engineering, Stanford University, Stanford, CA 94305 USA. He is now with the Department of Electrical Engineering and the Graduate Institute of Electronics Engineering, National Taiwan University, Taipei 10617, Taiwan, R.O.C.

Color versions of one or more of the figures in this letter are available online at http://ieeexplore.ieee.org.

Digital Object Identifier 10.1109/LPT.2007.904929

number of guided-wave approaches have also been investigated [4], [5]. Such an approach is usually preferred for on-chip interconnects since a waveguide receiver can be conveniently integrated with Si waveguides.

The recently demonstrated quantum-confined Stark effect (QCSE) [8] in Ge–SiGe quantum wells grown on Si opens up the possibility of realizing efficient electroabsorption modulators on silicon substrate [8], [9]. In this work, we utilize the QCSE to make quantum-well photodetectors. These detectors employ Ge–SiGe quantum wells and exhibit performance comparable to the aforementioned Ge and SiGe detectors. They have the additional advantage that quantum-well electroabsorption modulators can also be made using the same epitaxy. Our group demonstrated a novel side-entry modulator with a similar epitaxial structure as the detectors in this work [10]. Our design provides a convenient platform to realize photonic integrated circuits on silicon, and in particular CMOS-compatible on-chip optical interconnects.

II. DEVICE DESIGN AND FABRICATION

The SiGe is grown by reduced pressure chemical vapor deposition on a lightly p-doped silicon substrate. Si wafers are cleaned for 10 min in H_2SO_4 : H_2O_2 (4:1) at 90 °C, 10 min in H_2O : HCl : H_2O_2 (5:1:1) at 70 °C, and 30 s in H_2O : HF (50:1) before loading in the epi reactor. In the reactor, a 5-min 1100 °C hydrogen anneal is done before the actual growth to clean the native oxide. Subsequently, the SiGe growth starts with an 800-nm layer of B-doped Si_{0.1}Ge_{0.9}, grown in two stages at 500 °C, each of which is followed by a 750 °C–800 °C anneal, with a total anneal time of 40 min, to reduce the dislocation density and the surface roughness [9], [11]. Subsequently, a 90-nm spacer layer of undoped Si_{0.1}Ge_{0.9} is grown, which is then followed by $10 \text{ Ge}-\text{Si}_{0.16}\text{Ge}_{0.84}$ multiple quantum wells (MQWs). The ratio of the well and barrier thicknesses, 15 and 33 nm, respectively, is chosen so as to strain balance the superlattice overall with the relaxed $Si_{0.1}Ge_{0.9}$ buffer layer. Following the MQW layer, a 190-nm spacer layer of undoped $Si_{0.1}Ge_{0.9}$ and a 110-nm cap layer of As-doped $Si_{0.1}Ge_{0.9}$ are grown. The layer thicknesses are verified by secondary ion mass spectroscopy measurements. Temperature is a critical parameter to obtain high-quality SiGe epitaxy on Si and the optimum temperature for the growth is 400 °C-500 °C, which should not be exceeded in the process steps following the growth. Therefore, one possible way of realizing CMOS integration is carrying out the regular CMOS process steps up to and including ion implantation. The subsequent anneal to activate and diffuse the dopants, however, should be carefully designed considering the high-temperature anneals in the epi reactor. Following the

Manuscript received May 7, 2007; revised June 25, 2007. This work was supported by the Defense Advanced Research Projects Agency (DARPA)/ARO EPIC Program, and by the MARCO/DARPA FCRP Interconnect Focus Center.

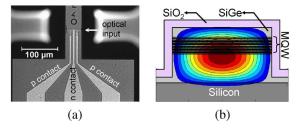


Fig. 1. (a) Plan view of a fabricated photodetector. (b) Schematic cross section and the principal optical mode of the waveguide.

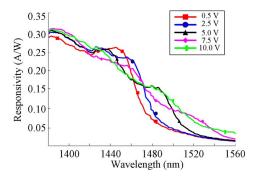


Fig. 2. External responsivity for TE modes in a 40- μ m detector.

SiGe growth, the remaining steps in the CMOS process can be finished.

Fig. 1(a) shows the plan view of a fabricated waveguide detector. The device fabrication starts with the lithographical definition of $3-\mu$ m-wide waveguides of lengths 20, 30, 40, 73, 113, and 163 μ m. The waveguides are realized by a $1.5-\mu$ m-deep ridge etch such that the etch stops within the B-doped Si_{0.1}Ge_{0.9} layer. Subsequently, 200 nm of SiO₂ is deposited to provide sidewall passivation. Following that, contact holes are opened and a Ti–Au metal contact layer is deposited and patterned using lift-off. Finally, 100- μ m-deep trenches are etched at the ends of the waveguide so that tapered single-mode fibers can be brought into proximity with the waveguide.

Fig. 1(b) shows the schematic of the waveguide cross section and the principal optical mode. In this multimode waveguide, the modes are confined by the SiGe–SiO₂ interfaces on the top and the sides, and by the SiGe–Si interface at the bottom. While the undoped Si_{0.1}Ge_{0.9} layers in the intrinsic region may contribute to the optical absorption through some remaining indirect absorption and through the Franz–Keldysh effect, the bulk of the absorption comes from the MQW region through the QCSE, which makes the overlap of the modes with the MQW region an important design parameter. In our design, the principal mode has a confinement (i.e., overlap) factor of 0.38.

III. EXPERIMENTAL RESULTS

The dark current is measured to be 7.2, 17.9, and 31.3 mA/cm^2 at biases of 0.5, 5, and 10 V, respectively. Low dark current indicates that the i-region is free of threading dislocations and has a low impurity concentration.

Fig. 2 shows the measured external responsivity, i.e., the photocurrent generated divided by the optical power in the fiber, for a transverse-electric (TE) mode in a 40- μ m waveguide. The band edge, which is around 1460 nm at zero bias, is red-shifted to 1500 nm as a reverse bias of 5 V is applied, without a

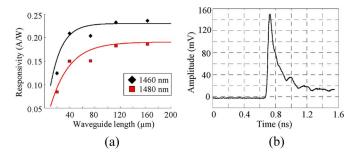


Fig. 3. (a) Responsivity versus waveguide length; (b) temporal response of a $163-\mu$ m waveguide photodetector. FWHM is measured to be 120 ps in response to a 1550-nm 100-fs pulse for a reverse bias of 8 V.

major decrease in responsivity. This shift without substantial broadening is a well-known characteristic of exciton peaks under QCSE in high-quality quantum-well structures. With appropriate bias, the responsivities are 260 mA/W at 1440 nm, 170 mA/W at 1480 nm, 84 mA/W at 1520 nm, and 44 mA/W at 1550 nm.

The external responsivity can be formulated as

$$R = \frac{\eta_i q \lambda \phi}{hc} \frac{\Gamma \alpha(\lambda, V)}{\Gamma \alpha(\lambda, V) + \alpha_i} \left(1 - \exp\left(-\left(\alpha_i + \Gamma \alpha(\lambda, V)\right)L\right)\right)$$
(1)

where η_i is the internal quantum efficiency, Γ is the overlap factor of the optical mode with the quantum wells, $\alpha(\lambda, V)$ is the absorption coefficient at wavelength λ and bias V, Lis the waveguide length, and ϕ is the coupling efficiency, including mode size mismatch and reflection [12]. α_i accounts for all the propagation losses that do not generate photocurrent. In our waveguide detectors, sidewall imperfections and refractive index nonuniformity in SiGe in the proximity of the bottom Si interface contribute to this kind of losses. Fig. 3(a) shows responsivity measurements for five different waveguide lengths with the theoretical curve overlaid. We used $\eta_i = 1$, $\Gamma = 0.38$, $\phi = 0.25$, $\alpha_i = 120$ cm⁻¹, and $\alpha(\lambda, V)$ was experimentally characterized by photocurrent measurements in surface-normal test structures.

Fig. 3(b) shows the temporal response of a 163- μ m photodetector to a 100-fs pulse at 1550 nm. A long waveguide was chosen for high responsivity in the long wavelength range. The full-width at half-maximum (FWHM) is measured to be 120 ps. The 3-dB bandwidth, however, is limited by the slow tail (500 ps at 10% of the peak) and is calculated to be 1.3 GHz. Fig. 4 shows the eye diagram at 2.5 Gb/s for a 1530-nm nonreturn-to-zero (NRZ) pseudorandom bit sequence, for which the output current is measured on a 50- Ω load resistance. We observe open eye diagrams, showing the feasibility of high-speed operation. The responsivity is limited in the long wavelength range, necessitating using relatively high power levels in the input optical signal (36 mW in fiber). Most of this light is not coupled in the waveguide [75% according to our fit in Fig. 3(a)] and such power levels apparently do not degrade the device performance.

It should be noted that QCSE is highly polarizationdependent in quantum-well structures [13], and these Ge–SiGe MQW photodetectors should be operated in the TE mode. That is because in transverse-magnetic (TM) modes only the light hole to conduction band transitions contribute to electroabsorption, and such transitions are apparently weak in this material

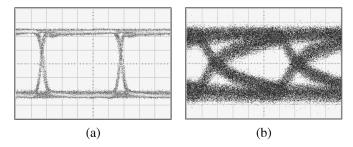


Fig. 4. The 2.5-Gb/s NRZ eye diagram for (a) the 1530-nm 15.3-dBm optical input and (b) the electrical output of a $163-\mu$ m device under 8-V reverse bias. (Horizontal 75 ps/div and vertical 5 mV/div for the electrical signal.)

system, not being well resolved in the spectra. While polarization dependence is a disadvantage, for an on-chip optical interconnect, the polarization has to be controlled in any case due to the polarization dependence of other components, such as electroabsorption modulators.

IV. DISCUSSION

From Fig. 3, the coupling loss is estimated to be 6 dB, which seems to be the major factor limiting the responsivity. The loss can be reduced by increasing the overlap integral of the input beam profile with the waveguide cross-section, and reducing facet reflections. Nevertheless, the detectors are primarily designed for on-chip optical interconnects and a fiber coupling will not be necessary in general.

Since the optimal absorption mechanism is from the quantum-well excitonic peaks, overlap of the modes with the quantum-well region is an important parameter. In the current design, the thick buffer layer occupies almost half of the total epitaxy, which reduces the mode coupling in the MQW region. A thinner buffer layer will increase the confinement factor, consequently increasing the responsivity.

The growth technique provides a convenient integration platform with the CMOS technology. However, a reverse bias above 5 V is required to achieve the desired responsivity for some wavelengths. It is possible to design the same MQW structure with thinner spacer regions and much thinner barriers with increased Si concentration, allowing for lower biases to achieve the desired electric field.

Employing a waveguide structure is advantageous in terms of real estate as well. Fig. 3 data suggests that there is not a substantial increase in responsivity for waveguides longer than \sim 50 μ m. Therefore, the waveguide structure will occupy much less area than many of the demonstrated detectors, which typically occupy \sim 1000 μ m².

V. CONCLUSION

In summary, we present compact, near-infrared detectors that employ Ge–SiGe quantum wells on silicon. This proof-of-principle demonstration leads us to anticipate the feasibility of high-speed operation and easy integration with silicon CMOS circuits as well as with the emerging on-silicon quantum-well electroabsorption modulator technology, making the MQW waveguide detector an attractive solution for on-chip optical interconnects.

ACKNOWLEDGMENT

The authors would like to thank T. Carver, T. Brand, and N. Cao, and Lawrence Semiconductor Research Laboratories O.F. acknowledges the Lucent Technologies Stanford Graduate Fellowship.

REFERENCES

- M. Jutzi, M. Berroth, G. Wohl, M. Oehme, and E. Kasper, "Ge-on-Si vertical incidence photodiodes with 39-GHz bandwidth," *IEEE Photon. Technol. Lett.*, vol. 17, no. 7, pp. 1510–1512, Jul. 2005.
- [2] A. K. Okyay, A. M. Nayfeh, K. C. Saraswat, T. Yonehara, A. Marshall, and P. C. McIntyre, "High-efficiency metal-semiconductor-metal photodetectors on heteroepitaxially grown Ge on Si," *Opt. Lett.*, vol. 31, pp. 2565–2567, 2006.
- [3] O. I. Dosunmu, D. D. Cannon, M. K. Emsley, L. C. Kimerling, and M. S. Unlu, "High-speed resonant cavity enhanced Ge photodetectors on reflecting Si substrates for 1550-nm operation," *IEEE Photon. Technol. Lett.*, vol. 17, no. 1, pp. 175–177, Jan. 2005.
- [4] L. Colace, G. Masini, A. Altieri, and G. Assanto, "Waveguide photodetectors for the near-infrared in polycrystalline germanium on silicon," *IEEE Photon. Technol. Lett.*, vol. 18, no. 9, pp. 1094–1096, May 1, 2006.
- [5] J. Liu, D. Pan, S. Jongthammanurak, K. Wada, L. C. Kimerling, and J. Michel, "Design of monolithically integrated GeSi electroabsorption modulators and photodetectors on an SOI platform," *Opt. Express*, vol. 15, no. 2, pp. 623–628, Jan. 2007.
- [6] Z. Huang, J. Oh, and J. C. Campbell, "Back-side-illuminated high-speed Ge photodetector fabricated on Si substrate using thin SiGe buffer layers," *Appl. Phys. Lett.*, vol. 85, no. 15, pp. 3286–3288, Oct. 2005.
- [7] D. A. B. Miller, D. S. Chemla, T. C. Damen, A. C. Gossard, W. Wiegmann, T. H. Wood, and C. A. Burrus, "Electric field dependence of optical absorption near the bandgap of quantum well structures," *Phys. Rev.*, vol. B32, pp. 1043–1060, 1985.
- [8] Y.-H. Kuo, Y. K. Lee, Y. Ge, S. Ren, J. E. Roth, T. I. Kamins, D. A. B. Miller, and J. S. Harris, "Strong quantum-confined Stark effect in germanium quantum-well structures on silicon," *Nature*, vol. 437, pp. 1334–1336, 2005.
- [9] Y.-H. Kuo, Y. K. Lee, Y. Ge, S. Ren, J. E. Roth, T. I. Kamins, D. A. B. Miller, and J. S. Harris, "Quantum-confined Stark effect in Ge/SiGe quantum wells on Si for optical modulators," *IEEE J. Sel. Topics Quantum Electron.*, vol. 12, no. 6, pt. 2, pp. 1503–1513, Nov./Dec. 2006.
- [10] J. E. Roth, O. Fidaner, R. K. Schaevitz, Y.-H. Kuo, T. I. Kamins, J. S. Harris, and D. A. B. Miller, "Optical modulator on silicon employing germanium quantum wells," *Opt. Express*, vol. 15, pp. 5851–5859, 2007.
- [11] A. Nayfeh, C. O. Chui, K. C. Saraswat, and T. Yonehara, "Effects of hydrogen annealing on heteroepitaxial-Ge layers on Si: Surface roughness and electrical quality," *Appl. Phys. Lett.*, vol. 85, pp. 2815–2817, 2004.
- [12] J. Shim, B. Liu, J. Piprek, and J. E. Bowers, "An improved approach of optical loss measurement using photocurrent and optical transmission in an electroabsorption modulator," *IEEE Photon. Technol. Lett.*, vol. 16, no. 6, pp. 1474–1476, Jun. 2004.
- [13] J. S. Weiner, D. A. B. Miller, D. S. Chemla, T. C. Damen, C. A. Burrus, T. H. Wood, A. C. Gossard, and W. Wiegmann, "Strong polarization-sensitive electroabsorption in GaAs/AlGaAs quantum well waveguides," *Appl. Phys. Lett.*, vol. 47, pp. 1148–1150, 1985.